


Resonant Confinement of an Excitonic Polariton and Ultraefficient Light Harvest in Artificial Photosynthesis

Yong-Cong Chen,^{1,*} Bo Song,² Anthony J. Leggett,³ Ping Ao,¹ and Xiaomei Zhu^{1,†}

¹Shanghai Center for Quantitative Life Sciences and Physics Department, Shanghai University, Shanghai 200444, China

²Shanghai Key Lab of Modern Optical System, School of Optical-Electrical Computer Engineering, University of Shanghai for Science and Technology, Shanghai 200093, China

³Shanghai Center for Complex Physics, Department of Physics and Astronomy, Shanghai Jiao Tong University, Shanghai 200240, China and Department of Physics, University of Illinois at Urbana-Champaign, Urbana, Illinois 61801, USA

 (Received 2 November 2018; revised manuscript received 25 February 2019; published 27 June 2019)

We uncover a novel phenomenon from a recent artificial light-harvesting experiment [P.-Z. Chen *et al.*, *Angew. Chem., Int. Ed. Engl.* **55**, 2759 (2016)] on organic nanocrystals of self-assembled difluoroboron chromophores. A resonant confinement of a polariton under strong photon-exciton coupling is predicted to exist within the microcavity of the crystal's own natural boundaries. Moreover, the radiative energy of a localized exciton falls into the spectrum of confinement. Hence, in the experiment, the spontaneous emission of an excited pigment would undergo a two-step process. It should first decay to an excitonic polariton trapped by the cavity resonance. The intermediate polariton could then funnel the energy directly to a doped acceptor, leading to the over 90% transfer efficiency observed at less than 1/1000 acceptor/donor ratio. The proposed mechanism is supported by parameter-free analyses entirely based on experiment data. Our finding may imply possible polariton-mediated pathways for energy transfers in biological photosynthesis.

DOI: [10.1103/PhysRevLett.122.257402](https://doi.org/10.1103/PhysRevLett.122.257402)

In the photosynthesis of plants and bacteria, the unusual high efficiency (over 95%) in the energy funneled from a large number of antenna chromophores to a single collector in the reaction center for the antenna has always attracted a great deal of research interest [1]. Away from the living cells, effort has been devoted to constructing artificial light-harvesting systems that can emulate the success of their natural counterparts. Recently, one such success based on nanocrystals of difluoroboron chromophores was reported by Chen *et al.* [2]. In the experiment, self-assembled nanocrystals of the β -diketonate (BF₂dfbk) derivative BF₂bcz (C₃₁H₂₅BF₂N₂O₂) with smooth surfaces and uniform sizes of 400–600 nm thickness and 5–7 μ m length [2,3] were used as the antenna (donors). Collecting agents (acceptors) coassembled in small ratios were molecules of similar structure, BF₂cna or BF₂dan, whose absorption spectra overlap with the emission spectrum of the donors. A donor excited by UV illumination was found to transfer the energy to a doped acceptor starting with a minute 10⁻⁶ acceptor/donor ratio and reaching 95% efficiency at less than 10⁻³ doping levels. A summary and further references [4,5] are presented in the Supplemental Material (SM) [6].

To explain the results by a diffusion-based mechanism would be difficult. In such a process, a localized Frenkel exciton would migrate to a nearby molecule via, e.g., Förster resonance energy transfer [7]. The transfer rate would be limited by the nature of the random walks and the relatively short exciton lifetime ($\tau \sim 3$ ns). The

room-temperature hopping time is typically picoseconds or longer [1,8,9]. Nevertheless, in the experiment $\sim 10\%$ energy transfer was observed at $\sim 10^{-6}$ acceptor/donor ratio. This would imply that an exciton needed to move $\sim 10^5$ steps with an average hopping time ~ 10 fs, 2 orders of magnitude faster than the typical scale. Hence the diffusion process could hardly account for the observed transfer efficiency. An alternative aggregate mechanism ought to exist in which the localized excitation should be converted into a form which propagates much faster than the Förster mechanism and is sufficiently long-lived.

We can also consider the opposite scenario, in which a Mott-Wannier exciton can propagate ballistically via an exciton band formed from the conduction and valence bands that exist in the periodic crystalline potential. Let us try to estimate the bandwidth or, equivalently, the nearest-neighbor hopping amplitude t_{exc} . The salient point here is that in organic crystals, in contrast to inorganic semiconductors, the HOMO- and LUMO-derived bands typically have a small dispersion, $\Delta E < 0.5$ eV, see, e.g., Refs. [10,11], corresponding to a value of the single-particle hopping amplitude $t_{\text{sp}} \sim \Delta E/2z < 0.07$ eV. Imagine an exciton which is originally formed on a particular site and tries to move to a nearest-neighbor site. It has two possible ways of doing so: a “single-step” process in which the electron and hole move simultaneously, and a two-step process in which (say) the electron moves first, leaving the hole behind, and the hole then

moves in a second step. In the two-step process, the energy deficit E_{int} in the intermediate state is essentially the binding energy of a localized Frenkel exciton, which, even taking into account screening through a dielectric constant ~ 3 , is no smaller than 0.3 eV (cf. Table 1 in Ref. [12]). Thus, the contribution to t_{exc} , $t_{\text{sp}}^2/E_{\text{int}}$, from this process is unlikely to exceed 0.015 eV. As is pointed out in Ref. [13], for so small a value of t_{exc} the motion at room temperature is likely to be strongly detuned (decohered) by the exciton-phonon coupling, which effectively recovers the Frenkel limit. It is more difficult to estimate the contribution of the single-step process. But on the basis of experimental and computational studies, Ref. [13] concludes that only in rather exceptional organic crystals transport by exciton motion is likely to be of the coherent (Mott-Wannier) type. While we cannot absolutely exclude this possibility, it looks distinctly improbable in the current context.

That leads us to the main proposal in this work: The sought-after aggregate mechanism may be provided by a resonance-induced exciton-polariton subject to self-confinement. In an organic (molecular) crystal, the exciton states across the entire crystal can interact coherently with the photons to form compound excitations known as exciton polaritons [14–16]. Polariton propagation has been reported in many organic crystal waveguides [17–20]. When the dimensions of a crystal is comparable to the photon wavelength, standing waves (SW) of polaritons become important. They can be trapped inside by total internal reflections at large $|\mathbf{k}|$ for the lower branch of the polariton’s dispersion is capped. As illustrated in Fig. 1, the trapped states fall into an excitonic region in which the photon composition is small. If a majority of the wave modes at the emission spectrum are captive, a confined polariton can serve as the intermediate state for a localized exciton undergoing spontaneous emission. The polariton can in turn be absorbed efficiently by a doped acceptor.

The conjectured “trapped exciton polariton” with the photon composition small is an ideal candidate to mediate the energy transfer. On one hand, the strong exciton-photon coupling reaches the order ~ 1 eV as a result of densely

packed donor molecules with a large dipole matrix element. This allows the photon field to induce a coherent response from the donor molecules across the entire crystal. The response can overcome the effects of static and/or dynamic disorder (~ 0.2 eV) in localizing the exciton. The hybrid modes then become the dominant channel to which a localized exciton can escape. This turns the propagation of the excited energy into a ballistic form. Though each polariton has a relatively small photon composition, the reduction to the spontaneous emission rate is offset by an increase in the number of large $|\mathbf{k}|$ modes. On the other hand, the smallness of the photon composition suppresses the “geometrical” leaking rate out of the nanocrystal as the group velocity of polaritons is also reduced. The long confinement time (~ 5 ps) is essential for a minute quantity of doped acceptors to compete against the leaking and achieve the high energy transfer rate.

There is a rich literature related to the key points of the current work, the exciton transfer and polariton confinement due to strong exciton-photon coupling in a microcavity. Theoretically, with the inclusion of optical cavities the exciton conductance [21,22] in certain organic materials can be dramatically enhanced. Polariton-assisted remote energy transfer under surface plasmons [23] and polariton-mediated long-range energy transfer in organic molecules [24] were explored. On the experimental side, strong couplings of organic molecules [20,25] or chlorosomes of photosynthetic bacteria [26] to the electromagnetic (EM) field confined by metallic mirrors or Bragg reflectors along with the polariton-mediated energy transfers [27] were reported. Some studies on vibronic effects [28–30] confirmed the polariton modes in the strong coupling regime.

Nevertheless, in the current work the microcavity, provided by the natural boundaries of the nanocrystal in question, is three dimensional with an abundance of modes. The submicron crystal dimensions play a critical role for the proper confinement of polaritons at the emission energy. A number of factors affecting and/or enhancing the lifetime of a captive polariton require close scrutiny. Ultimately our analysis is entirely based on experimental data with no fitting parameter.

We now proceed to justify the hypothesis. We will first show quantitatively how the resonant confinement arises inside the crystal based on a full quantum mechanical analysis. Consider the electromagnetic waves inside a rectangular isotropic dielectric medium $L_1 \sim L_2 \sim \lambda_e$, $L_3 \sim 10\lambda_e$, with $\lambda_e \approx 500$ nm being the (vacuum) wavelength of the exciton emission. The dimensions are chosen to resemble the nanocrystals used in the experiment. Let the electric field,

$$\mathbf{E}(\mathbf{r}, t) = \mathbf{U}_{\mathbf{k}\alpha}(\mathbf{r}) \cos(\omega_{\mathbf{k}} t), \quad \epsilon_b \omega_{\mathbf{k}}^2 = \mathbf{k}^2 c^2, \quad (1)$$

be a standing wave inside the cavity with the background relative permittivity ϵ_b excluding the contribution from the excitons. We have

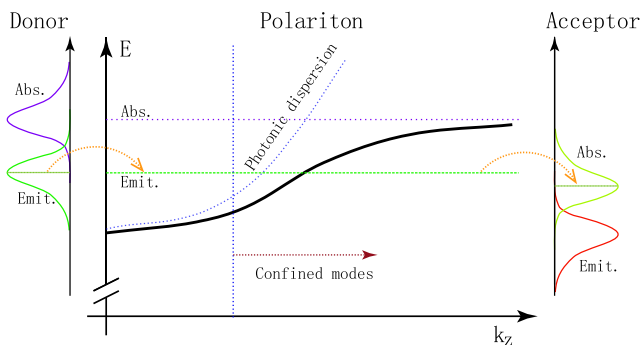


FIG. 1. Overlapping of the donor’s emission, the acceptor’s absorption, and the confined modes of the dispersion.

$$\begin{aligned} \mathbf{U}_{\mathbf{k}\alpha}(\mathbf{r}) &= (u_{x\mathbf{k}\alpha}U_{x\mathbf{k}}, u_{y\mathbf{k}\alpha}U_{y\mathbf{k}}, u_{z\mathbf{k}\alpha}U_{z\mathbf{k}}), \\ \mathbf{u}_{\mathbf{k}\alpha} &= (u_{x\mathbf{k}\alpha}, u_{y\mathbf{k}\alpha}, u_{z\mathbf{k}\alpha}), \quad \alpha = 1, 2, \end{aligned} \quad (2)$$

$$\begin{aligned} \mathbf{k} &= (\pi l_1/L_1, \pi l_2/L_2, \pi l_3/L_3), \quad l_i = 0, 1, 2, 3, \dots, \\ \tilde{\mathbf{k}} &= \mathbf{k}/|\mathbf{k}| = \mathbf{u}_{\mathbf{k}1} \times \mathbf{u}_{\mathbf{k}2}, \quad \mathbf{u}_{\mathbf{k}\alpha} \cdot \mathbf{u}_{\mathbf{k}\alpha'} = \delta_{\alpha\alpha'}, \end{aligned} \quad (3)$$

where $\mathbf{u}_{\mathbf{k}\alpha}$'s and \mathbf{k} are, respectively, the polarization and wave vectors. Explicit wave forms $U_{\gamma\mathbf{k}}(\mathbf{r})$ ($\gamma = x, y, z$) can be found in Ref. [31] and in the SM [6].

The standing waves Eq. (2) are in essence linear superpositions of 8 plane waves with mirror reflections of \mathbf{k} in some particular way. However, as the photon-exciton coupling turns on, the energy reduction in the lower branch of the hybrid entity can bound the EM field outside to the cavity surfaces, forming evanescent waves. A wave is trapped inside when, with \mathbf{k}_{\parallel} the tangent component of the wave vector, the inequality

$$\mathbf{k}_{\parallel}^2 c^2 > \epsilon_s (E_{\mathbf{k}}/\hbar)^2 \quad (4)$$

holds on all the surfaces. Here ϵ_s is the dielectric constant of the surrounding medium and $E_{\mathbf{k}}$ is the exciton-polariton energy. When a hybrid mode satisfies Eq. (4), it becomes isolated from and only weakly interacts with the surroundings. The confined state can be properly studied by including the evanescent waves as a whole, with a zero field boundary condition at infinity. As discussed in the SM [6], the wave forms Eqs. (S4) can reasonably represent the eigenstate of the electric field inside. In addition, we will neglect the surface component when the bulk of the exciton-photon coupling is considered. This implicitly sets the lower bound on the crystal dimensions for the analyses below to remain valid.

To obtain $E_{\mathbf{k}}$ we need a full quantum mechanical modeling of the electromagnetic interaction with the excitons [14–16]. To start with, one can quantize the macroscopic Maxwell equations using these eigenmodes. We shall not go through the full length of justification. For a given \mathbf{k} , the photon Hamiltonian and the electric field operator inside the cavity are given by (see, e.g., Ref. [32])

$$\hat{H}_{p\mathbf{k}} = \sum_{\alpha} \hbar\omega_{\mathbf{k}} \left(\hat{a}_{\mathbf{k}\alpha}^{\dagger} \hat{a}_{\mathbf{k}\alpha} + \frac{1}{2} \right), \quad (5)$$

$$\hat{\mathcal{E}}_{\mathbf{k}}(\mathbf{r}) = \sum_{\alpha} \mathcal{E}_{\mathbf{k}} (\hat{a}_{\mathbf{k}\alpha} + \hat{a}_{\mathbf{k}\alpha}^{\dagger}) \mathbf{U}_{\mathbf{k}\alpha}(\mathbf{r}), \quad (6)$$

where $\mathcal{E}_{\mathbf{k}} = \sqrt{\hbar\omega_{\mathbf{k}}/(2\epsilon_0\epsilon_b)}$ and the phase of $\hat{a}_{\mathbf{k}\alpha}$ is chosen for symmetric $\hat{\mathcal{E}}_{\mathbf{k}}(\mathbf{r})$.

The nanocrystals were illuminated by continuous UV light or weak laser pulses in time-resolved single photon counting measurements. The number of excitons in a

crystal at a given time is estimated to be very small (~ 10). Hence it suffices to consider the single exciton limit. We can approximate an excited molecule by a harmonic oscillator $\hat{b}, \hat{b}^{\dagger}$ restricted to its zeroth and first level, $E_1 = \hbar\omega_e \approx 2.5$ eV (for $\lambda_e \approx 500$ nm), namely the one excitation manifold. Let the position of the j th molecule be \mathbf{R}_j and the dipole matrix element between the ground and the excited states be $\mathbf{d} = \langle g|\hat{\mathbf{r}}|e\rangle$, then under a rotating wave approximation (e.g., Refs. [33–35]) we have the exciton-photon interaction Hamiltonian:

$$\begin{aligned} \hat{H}_{I\mathbf{k}} &= \sum_{j,\alpha} e\mathcal{E}_{\mathbf{k}} [\mathbf{U}_{\mathbf{k}\alpha}(\mathbf{R}_j) \cdot (\mathbf{d}^* \hat{b}_j^{\dagger} \hat{a}_{\mathbf{k}\alpha} + \mathbf{d} \hat{a}_{\mathbf{k}\alpha}^{\dagger} \hat{b}_j)], \\ [\hat{b}_i, \hat{b}_j^{\dagger}] &= \delta_{ij}, \quad i, j = 1, 2, \dots, N. \end{aligned} \quad (7)$$

By taking all molecules with the same matrix element, we have ignored the minor orientation difference between the two groups of molecules in the crystal.

Similar to Refs. [14–16,36], we can construct a standing-wave superposition of the identical electronic states from all the molecules:

$$\hat{b}_{z\mathbf{k}}^{\dagger} = \sqrt{\frac{V}{N}} \sum_j [U_{z\mathbf{k}}(\mathbf{R}_j) \hat{b}_j^{\dagger}], \quad (8)$$

$$|\phi_{z\mathbf{k}}\rangle = \hat{b}_{z\mathbf{k}}^{\dagger} |0\rangle, \quad [\hat{b}_{z\mathbf{k}}, \hat{b}_{z\mathbf{k}}^{\dagger}] = 1. \quad (9)$$

Two more SW states $|\phi_{x\mathbf{k}}\rangle$ and $|\phi_{y\mathbf{k}}\rangle$ can be likewise defined for the x and y components, respectively. The three SW states are mutually orthogonal (for large N), though SW states from different \mathbf{k} 's can overlap due to over-completeness of the constructions.

In terms of the coherent SW states [34,36], the non-interactive Hamiltonian for a given \mathbf{k} is

$$\hat{H}_{0\mathbf{k}} = \sum_{\gamma} \hbar\omega_e \hat{b}_{\gamma\mathbf{k}}^{\dagger} \hat{b}_{\gamma\mathbf{k}} + \sum_{\alpha} \hbar\omega_{\mathbf{k}} \hat{a}_{\mathbf{k}\alpha}^{\dagger} \hat{a}_{\mathbf{k}\alpha}, \quad (10)$$

and the interaction term Eq. (7) becomes

$$\hat{H}_{I\mathbf{k}} = \sum_{\alpha,\gamma} [g_{\mathbf{k}} \tilde{\mathbf{d}}_{\gamma}^* \cdot \mathbf{u}_{\mathbf{k}\alpha} \hat{b}_{\gamma\mathbf{k}}^{\dagger} \hat{a}_{\mathbf{k}\alpha} + \text{H.c.}], \quad (11)$$

$$g_{\mathbf{k}} = e|\mathbf{d}|\mathcal{E}_{\mathbf{k}}\sqrt{N/V}, \quad \tilde{\mathbf{d}}_{\gamma} = \mathbf{d}_{\gamma}/|\mathbf{d}|. \quad (12)$$

The scale of the exciton-photon interaction is crucial. From Table 1 of Ref. [3], a monomer in the DCM solution (CH_2Cl_2 , refractive index 1.42) has $\tau_f = 2.12$ ns, $\Phi_f = 0.80$ on the fluorescence lifetime and quantum yield, which translates to $|\mathbf{d}| \sim 2.0$ Å via the standard spontaneous emission rate formula. The crystal has 4 molecules in a unit cell of size 2823 Å³ (Table S2 of Supplemental Material in Ref. [2]); hence, $N/V = 1.4 \times 10^{-3}/\text{Å}^3$. At the resonance energy $\hbar\omega_{\mathbf{k}} = \hbar\omega_e$, $\epsilon_b \sim 2$, the coupling

constant $g_{\mathbf{k}}$ evaluates to ~ 0.8 eV. Note that by taking many parameters from the monomers in a solution, we implicitly assume that the crystalline electronic properties do not undergo significant changes upon self-assembly from the solution.

The photon-exciton coupling substantially exceeds the intermolecular dipole-dipole coupling. The contribution from the latter to the exciton dispersion was approximately calculated in Eq. (23) of Ref. [14]. The matrix element is diagonal but orientation dependent in the plane wave representation:

$$D_{\mathbf{k}} = \frac{Ne^2|\mathbf{d}|^2}{3\epsilon_0\epsilon_b V} [1 - 3|\tilde{\mathbf{k}} \cdot \tilde{\mathbf{d}}|^2]. \quad (13)$$

The coefficient evaluates to $0.35/\epsilon_b \approx 0.17$ eV. Since a standing wave is a composition of 8 plane waves over mirror reflections, the leading correction to $E_{\mathbf{k}}$ should be further reduced after averaging over the directions.

The two-state truncation employed above requires further scrutiny in the presence of local phonons. The latter are the low-lying vibrational modes associated with the electronic excitation. Their energy scale can be estimated from the Stokes shift $2\hbar\omega_s \approx 0.24$ eV in the fluorescence spectra (from Fig. S8 of Ref. [2]). In terms of the vertical transition picture, the ground state can be excited into a number of vibronic (an electronic plus a vibrational) states. Schematically, the Franck-Condon factor on the dipole element \mathbf{d} for the transition to the ν th vibrational mode $|\nu\rangle$ has the form

$$S_{\nu} = \exp(-S^2/2) \frac{S^{\nu}}{\sqrt{\nu!}} < 1, \quad (14)$$

where S is the Huang-Rhys parameter. We can introduce an effective excited state as a weighted superposition of all the vibrational states,

$$|e\rangle = \sum_{\nu} S_{\nu} |\nu\rangle, \quad (15)$$

which restores the transition dipole element back to its full oscillation strength. Furthermore, any other state orthogonal to Eq. (15) will have a vanishing dipole matrix element and, hence, will not be coupled to the photons. This justifies the two-state scheme provided that the energy spread of the vibronic states $\hbar\omega_s \ll g_{\mathbf{k}}$ and the effective excited state energy is elevated to $\hbar\omega_e + \hbar\omega_s$.

Finally, the Hamiltonian ($\hat{H}_{0\mathbf{k}} + \hat{H}_{I\mathbf{k}}$) from Eqs. (10) and (11) can be readily diagonalized. The details are presented in the SM [6], Eqs. (S15)–(S20). Under the criteria Eq. (S6), we are interested in where most captive modes reside and the corresponding energy drop $\Delta E_{\mathbf{k}} = \hbar\omega_e - E_{\mathbf{k}}$ from Eq. (S19), the photon composition factor A_{ph} from Eq. (S18), and the group velocity v_g from

Eq. (S20). The results illustrated in Fig. S1, with all parameters taken from the experiment, clearly confirm that the spontaneous emission indeed falls largely into the trapped modes with $\Delta E_{\mathbf{k}} \approx 2\hbar\omega_s$.

Going back to the main hypothesis, we next investigate the potential decay avenues once a polariton is trapped. An obvious path is the recapture of the polariton by another donor molecule. The process involves two competing factors, the large number of molecules N and a high thermal activation barrier $\sim 2\hbar\omega_s$ to overcome. An estimate from Eq. (S27) in the SM [6] gives the reabsorption rate $\Gamma_r \approx 9 \times 10^{-5} \omega_e$ at room temperature, a result to be revisited below.

Local phonons also induce stochastic fluctuations on physical properties such as the local excited energy. Since a coherent SW state is a superposition of the excited states across the entire crystal, their root mean square averages will be on the order of $1/\sqrt{N}$ ($\sim 2 \times 10^{-5}$). Thus their effects on the spectral broadening of the coherent polariton states are negligible.

The interactions with nonlocal lattice (acoustic) phonons can be significant. The exciton composition in a polariton can scatter with the latter via long-range dipolar fields. We can, nevertheless, estimate the effects from the attenuation data measured on a waveguide made of the same materials. The optical loss in Ref. [3] was found to be 0.033 dB/ μm on a $5 \times 5 \times 50$ μm crystalline rod, fabricated with the same material via a similar method. Taking an average group velocity $\sim c/(3\sqrt{\epsilon_b}) \approx c/4$, cf. Eq. (S20) [6], the light (567 nm) completes about 7 periods per μm , which gives a quality factor $Q \approx 0.6 \times 10^4$ or a decay time $\tau \sim 3$ ps. Since the value is an all-in-one result and is about the same as one would have obtained from the reabsorption alone, the damping by phonon scattering is likely not important in the current context.

For a dielectric cavity with dimensions close to the photon wavelength, the intrinsic factor limiting the resonance quality comes from the runaway of evanescent waves on the cavity surfaces, caused by surface curvatures or cavity edges (see, e.g., Ref. [37]). The off-surface decay length scales as $\sim (\mathbf{k}_{\parallel}^2 - \epsilon_s k_e^2)^{-1/2}$. Both the surface layer and more crucially the group velocity on the wave propagation should be significantly reduced as the photon composition gets smaller, which in turn heavily suppresses the leaking of the evanescent waves. Though a robust estimate remains a challenge, an indirect inference may be conducted here. The relevant analysis is carried out in Part D of SM [6], which gives an escape time $\tau \sim 5$ ps for the captive polariton, in line with reports in Refs. [3,17,38].

We can finally move on to the second part of the problem, namely to verify that our proposed mechanism can adequately account for the experimentally observed energy transfer rate. Doping of BF₂cna or BF₂dan creates a new escape path for the confined polariton. The transition is again bridged by the small photon composition $A_{\text{ph}} \sim 15\%$

in the captive mode. The transfer rate to acceptors Γ_a is calculated in Part E of SM [6]. A good estimate gives $\Gamma_a = \Gamma_0 \times (N_a/N)$, with N_a being the number of acceptors and $\Gamma_0 \approx \omega_e$. The linear dependence fits with the experimental observation.

Can the energy transfer rate be limited by the length of a nanocrystal when the group velocity is reduced and the escape time is short? Take a reasonable lower bound $v_g \approx c/10$ for an estimate. A polariton can travel over a $\sim 5 \mu\text{m}$ nanocrystal in $\sim 100 \times 2\pi/\omega_e \approx 0.2 \text{ ps} \ll 5 \text{ ps}$; hence it can reach any acceptor in the crystal. Needless to say, the crystal dimensions cannot be too small either as the evanescent waves, which do not interact with the acceptors, can become significant. Note that the transfer rate Γ_a competes against the escape rate Γ_p of the intermediate polariton out of confinement. 50% energy transfer from donors to acceptors should occur around $\Gamma_a \approx \Gamma_p$, which corresponds to $N_a/N \approx 0.6\Gamma_r/\Gamma_0 \approx 5 \times 10^{-5}$, in agreement with those reported in Fig. 3 of Ref. [2]. The parameter-free match extends to the entire doping range on the fluorescence decay measurement; see Part F of SM [6].

To summarize, both qualitative and quantitative analyses allow us to establish, to an excellent degree of confidence, that the self-confinement of excitonic polaritons is the likely mechanism behind the ultrahigh efficiency of energy transfer in the artificial light-harvesting system presented in Ref. [2]. Theoretical calculations based on the mechanism account for most of the observations reported. Other experiments based on organic nanocrystals, such as the one reported in Ref. [39], can possibly be explained via the same mechanism.

Can we test the hypothesis by further experiments? We propose that an infrared absorption measurement may be able to detect the possible transition from the lower to the higher branch of the dispersion. The latter will effectively kick a trapped polariton out of confinement. Hence, some abnormal profiles, in both the infrared absorption and the visible emission spectra, ought to show up when the crystals are placed under UV illumination. Finally, our study certainly raises an intriguing question: Can a similar resonant quantum confinement play a key role in the real photosynthesis? Namely, is it plausible that the entire block (s) of light-harvesting complexes forms a natural cavity to facilitate the efficient energy transfer? Some recent works have already looked into the polariton formation with the complexes [26,27,40].

This work was supported in part by the National Natural Science Foundation of China No. 16Z103060007 (P. A.).

* chenyongcong@shu.edu.cn

† Corresponding author.

xiaomeizhu@shu.edu.cn

- [1] T. Mirkovic, E.E. Ostroumov, J.M. Anna, R. van Grondelle, Govindjee, and G.D. Scholes, *Chem. Rev.* **117**, 249 (2017).
- [2] P.-Z. Chen, Y.-X. Weng, L.-Y. Niu, Y.-Z. Chen, L.-Z. Wu, C.-H. Tung, and Q.-Z. Yang, *Angew. Chem., Int. Ed. Engl.* **55**, 2759 (2016).
- [3] P.-Z. Chen, H. Zhang, L.-Y. Niu, Y. Zhang, Y.-Z. Chen, H.-B. Fu, and Q.-Z. Yang, *Adv. Funct. Mater.* **27**, 1700332 (2017).
- [4] S.N. Margar, L. Rhyman, P. Ramasami, and N. Sekar, *Spectrochim. Acta, Part A* **152**, 241 (2016).
- [5] H. Zhang and C. Liu, *Dyes Pigm.* **143**, 143 (2017).
- [6] See Supplemental Material at <http://link.aps.org/supplemental/10.1103/PhysRevLett.122.257402> for additional algebraic work and a comparison of the theory to experiment.
- [7] A. Ishizaki and G. R. Fleming, *Annu. Rev. Condens. Matter Phys.* **3**, 333 (2012).
- [8] W. Klöpffer, H. Bauser, F. Dolezalek, and G. Naundorf, *Mol. Cryst. Liq. Cryst.* **16**, 229 (1972).
- [9] N. Y. C. Chu, K. Kawaoka, and D. R. Kearns, *J. Chem. Phys.* **55**, 3059 (1971).
- [10] G. Koller, S. Berkebile, M. Oehzelt, P. Puschnig, C. Ambrosch-Draxl, F. P. Netzer, and M. G. Ramsey, *Science* **317**, 351 (2007).
- [11] M. Ohtomo, T. Suzuki, T. Shimada, and T. Hasegawa, *Appl. Phys. Lett.* **95**, 123308 (2009).
- [12] P. K. Nayak, *Synth. Met.* **174**, 42 (2013).
- [13] J. Arag and A. Troisi, *Adv. Funct. Mater.* **26**, 2316 (2016).
- [14] J. J. Hopfield, *Phys. Rev.* **112**, 1555 (1958).
- [15] S. Pekar, *J. Phys. Chem. Solids* **5**, 11 (1958).
- [16] A. S. Davydov, *Theory of Molecular Excitons*, 1st ed. (Springer, New York, 1971).
- [17] K. Takazawa, J.-i. Inoue, K. Mitsuishi, and T. Takamasu, *Phys. Rev. Lett.* **105**, 067401 (2010).
- [18] Q. H. Cui, Y. S. Zhao, and J. Yao, *Adv. Mater.* **26**, 6852 (2014).
- [19] T. Ellenbogen, P. Steinvurzel, and K. B. Crozier, *Appl. Phys. Lett.* **98**, 261103 (2011).
- [20] D. G. Lidzey, D. D. C. Bradley, M. S. Skolnick, T. Virgili, S. Walker, and D. M. Whittaker, *Nature (London)* **395**, 53 (1998).
- [21] J. Feist and F. J. Garcia-Vidal, *Phys. Rev. Lett.* **114**, 196402 (2015).
- [22] J. Schachenmayer, C. Genes, E. Tignone, and G. Pupillo, *Phys. Rev. Lett.* **114**, 196403 (2015).
- [23] M. Du, L. A. Martinez-Martinez, R. F. Ribeiro, Z. Hu, V. M. Menon, and J. Yuen-Zhou, *Chem. Sci.* **9**, 6659 (2018).
- [24] R. Sáez-Blázquez, J. Feist, A. I. Fernández-Domínguez, and F. J. García-Vidal, *Phys. Rev. B* **97**, 241407(R) (2018).
- [25] R. J. Holmes and S. R. Forrest, *Phys. Rev. Lett.* **93**, 186404 (2004).
- [26] D. Coles, L. C. Flatten, T. Sydney, E. Hounslow, S. K. Saikin, A. Aspuru-Guzik, V. Vedral, J. K.-H. Tang, R. A. Taylor, J. M. Smith, and D. G. Lidzey, *Small* **13**, 1701777 (2017).
- [27] D. M. Coles, Y. Yang, Y. Wang, R. T. Grant, R. A. Taylor, S. K. Saikin, A. Aspuru-Guzik, D. G. Lidzey, J. K.-H. Tang, and J. M. Smith, *Nat. Commun.* **5**, 5561 (2014).

- [28] J. A. Ćwik, S. Reja, P. B. Littlewood, and J. Keeling, *Europhys. Lett.* **105**, 47009 (2014).
- [29] N. Wu, J. Feist, and F. J. Garcia-Vidal, *Phys. Rev. B* **94**, 195409 (2016).
- [30] F. Herrera and F. C. Spano, *Phys. Rev. Lett.* **116**, 238301 (2016).
- [31] P. M. Morse and H. Feshbach, *Methods of Theoretical Physics. Part II* (McGraw-Hill, New York, 1953), Chaps. 9–13.
- [32] K. Kakazu and Y. S. Kim, *Phys. Rev. A* **50**, 1830 (1994).
- [33] E. T. Jaynes and F. W. Cummings, *Proc. IEEE* **51**, 89 (1963).
- [34] K. Hepp and E. H. Lieb, *Ann. Phys. (N.Y.)* **76**, 360 (1973).
- [35] J. Keeling, P. R. Eastham, M. H. Szymanska, and P. B. Littlewood, *Phys. Rev. Lett.* **93**, 226403 (2004).
- [36] R. H. Dicke, *Phys. Rev.* **93**, 99 (1954).
- [37] G. M. Wysin, *J. Opt. Soc. Am. B* **23**, 1586 (2006).
- [38] M. I. Sluch, A. S. Averjushkin, O. I. Tolstikhin, and A. G. Vitukhnovsky, *Phys. Scr.* **50**, 585 (1994).
- [39] M.-J. Sun, Y.-W. Zhong, and J. Yao, *Angew. Chem., Int. Ed. Engl.* **57**, 7820 (2018).
- [40] Z. Zhang, P. Saurabh, K. E. Dorfman, A. Debnath, and S. Mukamel, *J. Chem. Phys.* **148**, 074302 (2018).